Stability analysis of real-time dynamic substructuring using delay differential equation models

M. I. Wallace[1,*], J. Sieber[1], S. A. Neild[1], D. J. Wagg[1] and B. Krauskopf[1]

[1] *Bristol Laboratory for Advanced Dynamics Engineering, University of Bristol, Queen's Building, Bristol BS8 1TR, UK*

SUMMARY

Real-time dynamic substructuring is an experimental technique for testing the dynamic behaviour of complex structures. It involves creating a hybrid model of the entire structure by combining an experimental test piece — the substructure — with a numerical model describing the remainder of the system. The technique is useful when it is impractical to experimentally test the entire structure or complete numerical modelling is insufficient.

In this paper we focus on the influence of delay in the system, which is generally due to the inherent dynamics of the transfer systems (actuators) used for structural testing. This naturally gives rise to a delay differential equation (DDE) model of the substructured system. With the case of a substructured system consisting of a single mass-spring oscillator we demonstrate how a DDE model can be used to understand the influence of the response delay of the actuator. Specifically, we describe a number of methods for identifying the critical time delay above which the system becomes unstable.

Because of the low damping in many large structures a typical situation is that a substructuring test would operate in an unstable region if additional techniques were not implemented in practice. We demonstrate with an adaptive delay compensation technique that the substructured mass-spring oscillator system can be stabilized successfully in an experiment. The approach of DDE modelling also allows us to determine the dependence of the critical delay on the parameters of the delay compensation scheme. Using this approach we develop an over-compensation scheme that will help ensure stable experimental testing from initiation to steady state operation. This technique is particularly suited to stiff structures or those with very low natural damping as regularly encountered in structural engineering.

KEY WORDS: Substructuring; hybrid testing; delay differential equations; delay compensation.

1. INTRODUCTION

The hybrid numerical-experimental testing technique known as *real-time dynamic substructuring* allows one to observe at full scale the behaviour of a critical element under dynamic loading. The whole system under consideration — the emulated system — is split up into an experimental test piece — the substructure — and a numerical model describing the

*Correspondence to: M. I. Wallace, **max.wallace@bristol.ac.uk**

remainder of the structure. The challenge is to ensure that the substructure and the numerical model together behave in the same way as the emulated system. This procedure is useful when testing large scale civil engineering structures under extreme dynamic loading, such as earthquakes, because critical components can be tested at full scale. This avoids problems with scaling effects for problematic material such as reinforced concrete [1].

An overview of substructuring and how it relates to the field of experimental laboratory testing of large structures is given by Williams and Blakeborough [2]. So far the technique has been developed successfully by using expanded time scales, known as pseudo-dynamic testing [3–9], with the limitation that dynamic and hysteresis forces must be estimated. Implementing the substructuring process in real-time eliminates the need for these estimations and has been the subject of much recent research [10–15]. To carry out a substructuring test, the component of interest is identified as the substructure and fixed into an experimental test system. To link the substructure to the numerical model of the remainder of the system, a set of *transfer systems* (that act on the substructure) are controlled to follow the appropriate output from the numerical model [16–19]. A transfer system is typically a single (electric or hydraulic) actuator with its proprietary controller, but may also be a more complex test facility, such as a shaking table. At the same time, the forces between the transfer systems and the substructure are fed back as inputs to the numerical model. This entire process must take place in real-time.

The focus of this paper is on the fundamental principles behind substructuring. Our aim is to develop an understanding of the *effect of delay errors* that are always present in a substructured system. Delays arise naturally, because it is not possible for any transfer system to react instantaneously to a change of state as prescribed by the numerical model. In some situations the transfer system delay may be so small as to be negligible, but the typical situation in substructuring is that this delay is large enough to have a significant influence on the overall dynamics of the substructured system.

The method we employ here is to model the substructured system with *delay differential equations* (DDEs), which are derived from the ODE model of the system by explicitly including the delay(s) due to the transfer system(s). A DDE model is a system of differential equations that depend on the current state of the system and on the state of the system some fixed time τ ago. (We focus in this paper on the case of a single fixed delay, but it is also possible in this framework to consider multiple fixed delays as commonly found in multi-actuator experiments.) The advantage of DDE modelling is that we can use powerful analytical and numerical methods to determine the stability of the DDE model and, hence, of the substructured system. Specifically, the loss of stability as a function of increasing delay is observed in a substructured system by the onset of oscillations. Because this corresponds in the DDE model to a pair of complex conjugate eigenvalues with zero real part, it is possible to determine the critical delay, τ_c, above which the system is unstable.

To illustrate this general approach we introduce in Section 2 the example of a substructured single mass-spring oscillator that we use throughout. We concentrate on the case of a system with very low damping as typically arises in structural dynamics. We identify the origin of the delay in terms of the transfer system and show how it appears in the feedback force from the substructure. As the first step, we determine in Section 3 the critical delay τ_c of the system. Because the system is linear and quite simple, we compute explicit expressions for τ_c by computing the purely imaginary complex roots directly from the characteristic equation [20, 21]. We then demonstrate how the stability regions can be computed numerically with the mathematical tool DDE-BIFTOOL [22]. Because this software does not require any

special property of the governing equations, the section demonstrates how one can find τ_c in a general situation of more complex and nonlinear substructured systems.

For a substructured system to be stable the delay due to the transfer system must be less than τ_c. This is often not the case so it is common to apply a delay compensation scheme to negate the effect of the transfer system delay [10,13,23]. In Section 4 we use a generic approach to delay compensation, presented by Wallace *et al.* [19], to authenticate the approach proposed in this paper with experimental data. Finally, in Section 4.1 we use information gained from the DDE modelling to propose a method of over-compensation that can be used to help attain a successful real-time dynamic substructure test especially suited to dynamical systems with very low damping.

2. THE SUBSTRUCTURED SYSTEM

We consider the example of a single mass-spring oscillator system with one excitation input, r, shown in Figure 1, for the emulated system. The state of the system is represented by z^*, where $(.)^*$ indicates that these dynamics are based on the 'complete' dynamics of this emulated system.

In order to create a substructured model of the system shown in Figure 1, the spring k_s is isolated and taken to be the substructure. The remainder of the structure, the excitation wall and the mass-spring-damper unit, is modelled numerically. This decoupling results in the substructured system shown schematically in Figure 2. The dynamics of the numerical model are governed by

$$m\ddot{z} + c(\dot{z} - \dot{r}) + k(z - r) = F, \tag{1}$$

where the feedback force F is the substructure response of $F = -k_s x$ (see Figure 2). As the transfer system has its own dynamics, it cannot react instantaneously to the change of state of the numerical model and thus introduces an inevitable time delay. This means that $x(t) = z(t - \tau)$ for some positive τ. In our modelling we take τ to be constant and ignore the additional effects of any physical disturbances on the transfer system.

The delay τ introduces a systematic synchronisation error $z(t) - x(t) = z(t) - z(t - \tau)$ into the substructuring algorithm. Wallace *et al.* [19] have conjectured that, in general, the

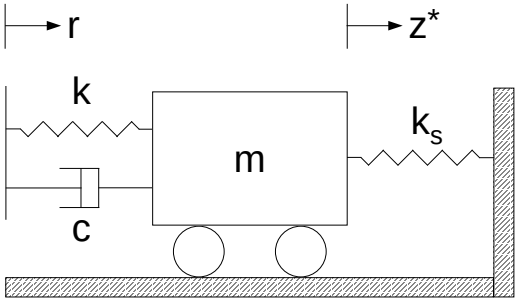

Figure 1. Schematic representation of the single mass-spring oscillator

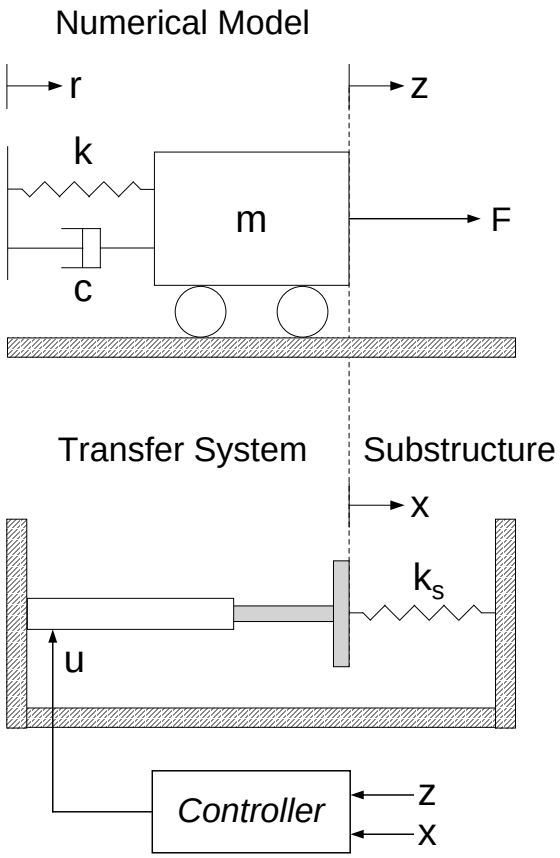

Figure 2. Schematic representation of a *substructured* system with one transfer system. State variable for the Numerical Model: $z(t)$, state variable for the Transfer System: $x(t)$, control input to actuator (voltage): $u(t)$.

substructured system $z(t)$ approximates the emulated system $z^*(t)$ if this synchronisation error is small, that is, $z \to z^*$ if $x \to z$. Therefore, it is natural that the synchronisation error is a crucial measure for the accuracy of the substructuring experiment and, in fact, may be the only explicit measurement of accuracy available for complex systems. We call the substructured system *unstable* if the synchronisation error grows exponentially in time and we call it *stable* if the synchronisation error remains bounded. As a result, when the synchronisation error is non-zero, the force is also described by the same delayed state z of the numerical model, such that $F = -k_s z(t-\tau)$. The overall substructured system is then governed by a delay differential equation (DDE) that can be written as

$$m\ddot{z} + c\dot{z} + kz + k_s z(t-\tau) = c\dot{r} + kr\,. \tag{2}$$

3. STABILITY OF THE SUBSTRUCTURED SYSTEM

3.1. Explicit Stability Analysis

Using Equation (2) with $r = \dot{r} = 0$ and $x(t) = z(t-\tau)$ we obtain the complimentary equation

$$m\ddot{z} + c\dot{z} + kz + k_s x = 0. \tag{3}$$

This can be expressed with non-dimensionalized parameters as

$$\frac{d^2 z}{d\hat{t}^2} + 2\zeta\frac{dz}{d\hat{t}} + z + px = 0, \tag{4}$$

where

$$\omega_n = \sqrt{\frac{k}{m}}, \qquad \hat{t} = \omega_n t, \qquad \hat{\tau} = \omega_n \tau, \qquad p = \frac{k_s}{k}, \qquad \zeta = \frac{c}{2\sqrt{mk}}.$$

(The values of these parameters are given in Section 4.)

The introduction of a delay term into a linear ordinary differential equation (ODE) has two effects. First, it changes the spectrum of the ODE by a perturbation of order τ and secondly it introduces infinitely many new modes. Searching for solutions of the form $z = Ae^{\lambda\hat{t}}$ in Equation (4) leads to the characteristic equation

$$\lambda^2 + 2\zeta\lambda + 1 + pe^{-\lambda\hat{\tau}} = 0, \tag{5}$$

where complex roots λ_i are the system eigenvalues. If the delay is small, the new modes are all strongly damped and the perturbation of the ODE spectrum can be expanded by approximating $e^{\lambda\hat{\tau}} = (1 - \lambda\hat{\tau})$ to give a critical delay value of

$$\tau_c = \frac{2\zeta}{p\omega_n} = \frac{c}{k_s}. \tag{6}$$

This expression highlights that lightly damped stiff structures, such as those commonly encountered in structural engineering, will have a small τ_c and, consequently, it will be more difficult to maintain stability of the substructuring test. A previous analysis of the effect of time delay in substructuring [10] used an energy analysis of periodic orbits to equate the time delay to a form of negative damping. Equation (6) demonstrates how this negative damping manifests itself. In fact, the equivalent negative damping term can be expressed as $c_{neg} = -k_s\tau$, with instability occurring at the point of sign change for the damping of the overall system.

In order to determine the stability boundaries of Equation (4) explicitly we search for points in the parameter space where its characteristic equation has purely imaginary solutions, that is, just undergoes a Hopf bifurcation; entailing the creation of (small) oscillations and is a well know phenomenon in the context of DDEs [21, 24]. This analysis is valid not just for small τ but for any value of τ [25, 26]. Specifically, the stability boundaries are found in the parameter space by searching for solutions of the form $z = Ae^{j\omega t} = Ae^{j\hat{\omega}\hat{t}}$ where $\hat{\omega} = \frac{\omega}{\omega_n}$ is a positive real number (0 cannot be a characteristic root in this case). We insert $\hat{\omega}$ into the characteristic equation (5) to obtain a system of two real equations:

$$0 = 1 - \hat{\omega}^2 + p\ \cos(\hat{\omega}\hat{\tau}) \qquad \text{for the real part,} \tag{7}$$

$$0 = 2\zeta\hat{\omega} - p\ \sin(\hat{\omega}\hat{\tau}) \qquad \text{for the imaginary part.} \tag{8}$$

We use the Equations (7) and (8) to express the parameters as functions of $\hat{\omega}$. In this way, we can identify all points in the parameter space where the DDE has purely imaginary eigenvalues and, thus, changes stability at a Hopf bifurcation. Taking into account that the cot function is periodic and p and ζ must be positive we get

$$\hat{\tau} = \frac{1}{\hat{\omega}} \operatorname{arccot}\left(\frac{\hat{\omega}^2 - 1}{2\zeta\hat{\omega}}\right) + \frac{2\mathrm{n}\pi}{\hat{\omega}}, \tag{9}$$

where n is an integer, is satisfied on the stability boundary. If arccot is to be taken between 0 and π then n has to be non-negative since $\hat{\tau}$ is positive. Squaring and adding the Equations (7) and (8) and rearranging for p, we get

$$p = \sqrt{(\hat{\omega}^2 - 1)^2 + 4\zeta^2\hat{\omega}^2}. \tag{10}$$

Figure 3(a1) shows the curves for $n = 0$ to $n = 2$ (up to the limit of $\hat{\tau} \approx 12.79$, or $\tau = 0.4$s) of the infinite solution set for the critical parameter pairs $(\hat{\tau}, p)$ in the $(\hat{\tau}, p)$-plane with ζ fixed at 0.0213. These curves are parameterized by $\hat{\omega}$ running from 0 to $+\infty$ in Equations (9) and (10). Along these curves the system has a pair of purely imaginary eigenvalues and, hence, gains one additional unstable mode. Along the line $\hat{\tau} = 0$ the system is stable. Consequently, always the lowest parts of the curves define the stability boundary; the grey area is the region of stability. For comparison we have inserted into Figure 3(a1) as a dashed curve the stability boundary obtained from the perturbation (approximate) analysis Equation (6). As stated earlier, it can be seen that the approximation only holds for small values of the delay. Further more it is a slight underestimation of the explicit solution as the higher order terms are not included in the approximation. Figure 3(a2) shows an enlargement of the region where the ratio of the spring constants has a value of $p = 1$ for which the experimental testing is performed in Section 4. The non-dimensionalized critical value $\hat{\tau}_c$ can be read off as $\hat{\tau}_c = 0.04627$, from which the critical time delay can be computed as $\tau_c = 1.335\,\mathrm{ms}$.

To obtain the critical delay $\hat{\tau}_c$ and ζ for fixed p as parametric curves in the $(\hat{\tau}, \zeta)$-plane we rearrange Equation (7) for $\hat{\tau}$ and (10) for ζ, thus expressing the critical $\hat{\tau}$ and ζ as functions of $\hat{\omega}$ and p (taking into account that $\hat{\tau}$ and ζ must be positive):

$$\hat{\tau} = \frac{1}{\hat{\omega}} \arccos\left(\frac{\hat{\omega}^2 - 1}{p}\right) + \frac{2n\pi}{\hat{\omega}}, \tag{11}$$

$$\zeta = \frac{1}{2\hat{\omega}}\sqrt{p^2 - (\hat{\omega}^2 - 1)^2}, \tag{12}$$

where $\hat{\omega}$ runs from $\sqrt{\max\{0, 1-p\}}$ to $\sqrt{1+p}$, and n is any non-negative integer if arccos takes values between 0 and π. Figure 3(b1) shows the stability region (grey) and the critical values of $\hat{\tau}$ and ζ for fixed $p = 1$ using the curves defined parametrically by (11) and (12). The primary curve with $\hat{\tau}$ for $n = 0$ is always the stability boundary in the $(\hat{\tau}, \zeta)$-plane. Again, we have inserted into Figure 3(b1) as a dashed curve the approximate stability boundary given by Equation (6) that was obtained from perturbation analysis. This curve is only accurate for systems which are lightly damped with a maximum of approximately 15% damping for this structure, which can be seen from the enlargement of the experimental region in Figure 3(b2). Figures 3(a1) and 3(b1) also highlight that there are 'stable' parameter regions. These are regions where the system is stable regardless of the delay $\hat{\tau}$. We note that the vast majority of structures, especially in the civil engineering field, are lightly damped such that operating

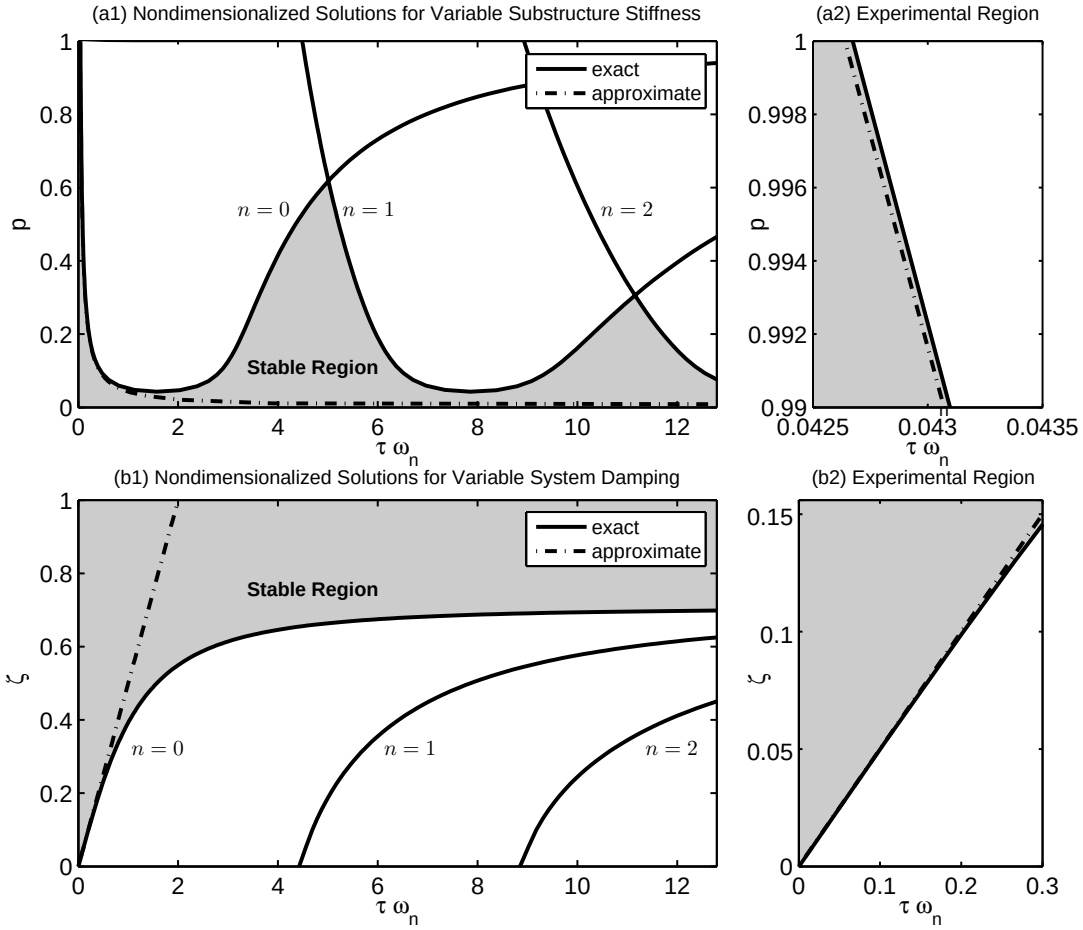

Figure 3. Non-dimensionalized Hopf stability boundaries of the DDE (4) for variable response delay. Fixed parameters: $\zeta = 0.0213$ in panels (a) and $p = 1$ in panels (b).

in the region of stability for all $\hat{\tau}$ would be extremely unlikely. However, when substructuring mechanical components, such as individual damper units, other parts of the stable region are likely to be accessible.

Additionally, we note that the frequency at which instability occurs is constant and independent of the excitation frequency. We can find the instability frequency, ω_I, from Equation (10) by rearranging for $\hat{\omega}$ for the case where $p = 1$ and $\zeta = 0.0213$ at the point of instability,

$$\omega_I = \omega_n \sqrt{(2 - 4\zeta^2)^2} = 7.116 Hz. \tag{13}$$

3.2. Numerical Stability Analysis

For more complex DDEs than Equation (4) it may become impossible to find stability regions as shown in Figures 3 by analytical calculations. We therefore move to a numerical approach for finding the stability regions when the substructured system is complex or nonlinear. In this section, we use a mathematical tool called DDE-BIFTOOL to demonstrate how this numerical analysis may be applied. DDE-BIFTOOL is a collection of Matlab routines for numerical bifurcation analysis of systems of DDEs with multiple fixed, discrete delays and is freely available for scientific purposes [22].

We used DDE-BIFTOOL to find the critical delay τ_c where the first Hopf bifurcations occurs

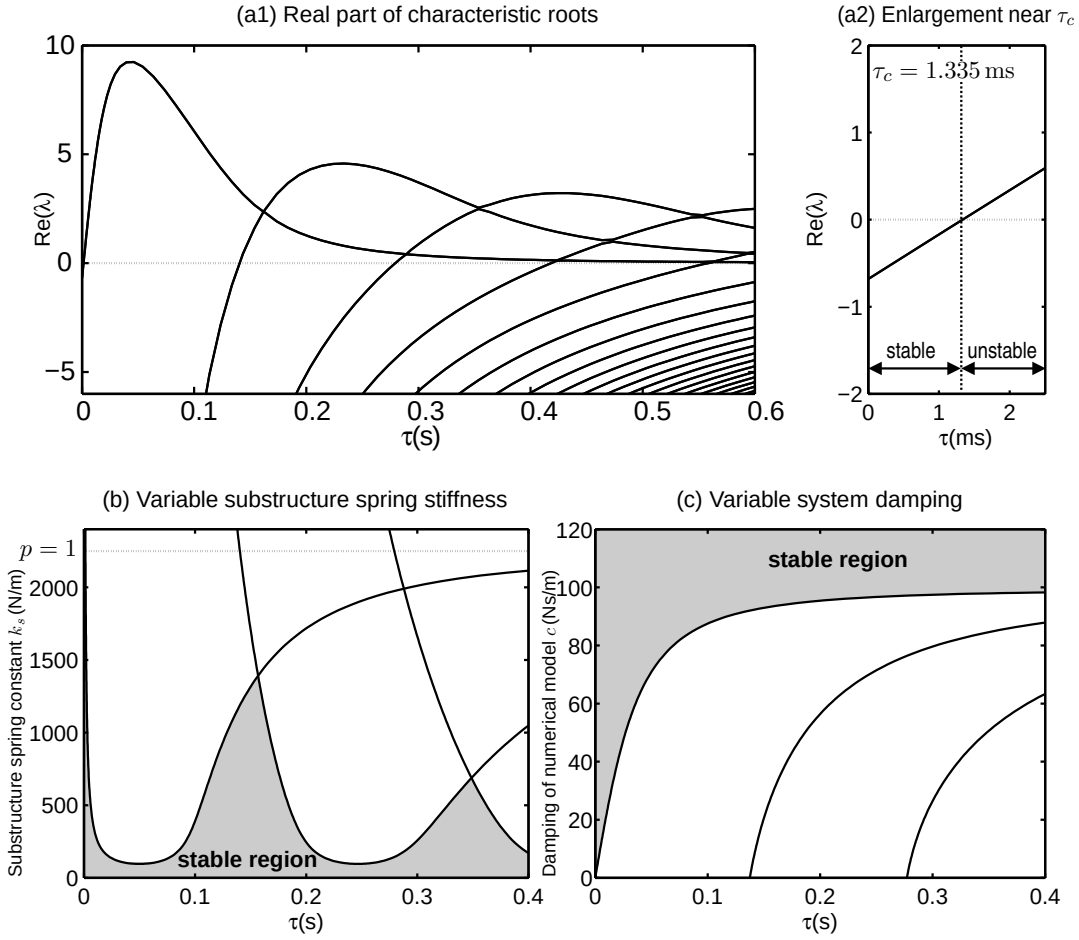

Figure 4. (a1) Real part of complex roots of the substructured system computed using DDE-BIFTOOL with enlargement of the critical region (a2). Hopf bifurcation diagram showing the stability region for, (b) variable substructure spring stiffness k_s (c = 3Nm/s), and (c) variable system damping c (k_s = 2250N/m). Other system parameters: m = 2.2kg and k = 2250N/m.

and the substructured system destabilizes. Figure 4(a1) shows the real parts of the roots of the characteristic equation for the substructured system as the delay τ is increased (shown up to $\tau = 0.6$s). The system is stable when all roots are in the left half plane, that is, none of the curves are above zero. The first Hopf bifurcation takes place when the dominant branch crosses the dashed line where $\mathrm{Re}(\lambda) = 0$. As can be observed from the enlarged view in Figure 4(a2), stability is maintained until the response delay reaches the critical value of $\tau_c = 1.335$ms. This agrees with the value found in the explicit stability analysis in Section 3.1.

The zero roots can be followed to see the effect of varying the structural parameters on the stability of the substructured system in terms of the critical delay. Figure 4(b) shows the stability boundary given by τ_c when the spring stiffness is varied. As expected, the boundary obtained with DDE-BIFTOOL agrees with that in Figure 3(a1). For the response time of the actuator of the experiments presented in Section 4 we are dealing with a small delay, so that the first Hopf curve in Figure 4(c) is the relevant stability boundary. Figure 4(c) shows the stability region, bounded by τ_c, for changing system damping of the numerical model. Again, we have agreement with the result found from the characteristic equation shown in Figure 3(b1).

Overall, the results in this section agree with the explicit stability analysis in Section 3.1. This demonstrates the potential of the numerical stability analysis with DDE-BIFTOOL, with the added advantage that it works also for much more complex and nonlinear systems.

4. EXPERIMENTAL SUBSTRUCTURE TESTING WITH DELAY COMPENSATION

To implement real-time dynamic substructuring experimentally we used a dSpace DS1104 R&D Controller Board running on hardware architecture of MPC8240 (PowerPC 603e core) at 250 MHz with 32 MB synchronous DRAM. This is fully integrated into the block diagram-based modelling tool MATLAB$^{\mathrm{TM}}$/Simulink$^{\mathrm{TM}}$which is used to build the substructured model. The dSpace companion software ControlDesk is used for online analysis, providing soft real-time access to the hard real-time application. The structural system parameters were found through system identification to be spring stiffness $k = k_s = 2250$N/m and damping ratio $c = 3$Ns/m. The constant mass of 2.2kg is connected via three parallel shafts that constrains its motion to one degree of freedom. The transfer system is a UBA (timing belt and ball screw) linear Servomech actuator. Figure 5 shows the Experimental rig setup of the substructured system.

Focusing on the fundamental principles of delay errors and the concepts proposed by the DDE modelling we now perform small scale tests using a servo-mechanical actuator. As the system considered is very lightly damped, $\zeta = 0.0213$, we must employ a control strategy to ensure the stability of the substructuring algorithm as the transfer system delay τ will be greater than the critical delay value of $\tau_c = 1.335$ms. A common strategy in real-time substructuring is delay compensation by extrapolation [10,16,19,23] which has been shown to work on both servo-hydraulic and servo-mechanical actuators. The technique used in this paper is the Adaptive Forward Prediction (AFP) algorithm, presented by Wallace *et al.* [19], which is based on the idea of feeding a forward prediction z' of the state z of the numerical model into the transfer system. It is a generic approach to delay compensation as it allows non-integer multiples of the previous time step to be predicted and adapts to changing plant conditions through self-tuning. The AFP algorithm uses the prediction $z(t)' = (P_{N,n,\Delta}[z])(t + \rho)$ where $P_{N,n,\Delta}[z]$ is the least squares fitting N^{th}-order polynomial through the n time-point pairs

Figure 5. Experimental rig setup of substructured system.

$(t, z(t))$, $(t-\Delta, z(t-\Delta))$,..., $(t-(n-1)\Delta, z(t-(n-1)\Delta))$. The time difference Δ is the sampling time step (1ms for experimentation) and ρ is the amount of forward prediction. Thus, ρ is used to compensate for the delay τ generated by the control of the transfer system, which we do not know prior to experimentation.

Figure 6 shows the experimental results for a wall excitation of 3Hz and constant delay compensation of $\rho = 9.4$ms with polynomial fitting paraments $N = 4$ and $n = 16$. It can be seen from Figure 6(a) that the numerical model dynamics z closely replicate those of the emulated system z^*, losing accuracy only slightly at the direction changes of the actuator. Note that the transfer system dynamics are not shown on this plot but are represented by a synchronisation subspace plot [27] in Figure 6(b). Perfect synchronisation is represented by a straight diagonal line. A constant delay turns this straight line into an ellipse, as can be seen from the limit of stability shown in grey representing z vs. $z(t-\tau_c)$. We can see from the subspace plot that there is generally a high level of synchronisation, below the stable limit, apart from when the actuator changes direction. Here we observe a region of loss in accuracy as the control signal must reach a certain level to overcome the static friction of the actuator mechanics before the piston will move. In fact, the algorithm verges into the unstable region at both limits. However, despite this, once the static friction is overcome, synchronisation is quickly regained. This shows that the instability shown by a substructured system (or this type of DDE) is not catastrophic. For instability to grow cumulatively, the synchronisation must remain in the unstable region for a number of successive time steps. Therefore, if the control algorithm can recover more quickly than the exponential growth, then the system will be able to recover regardless of the disturbance to the synchronisation. We note that the lower the damping in the system, the smaller the critical limit of stability and the faster instability will grow for a given delay.

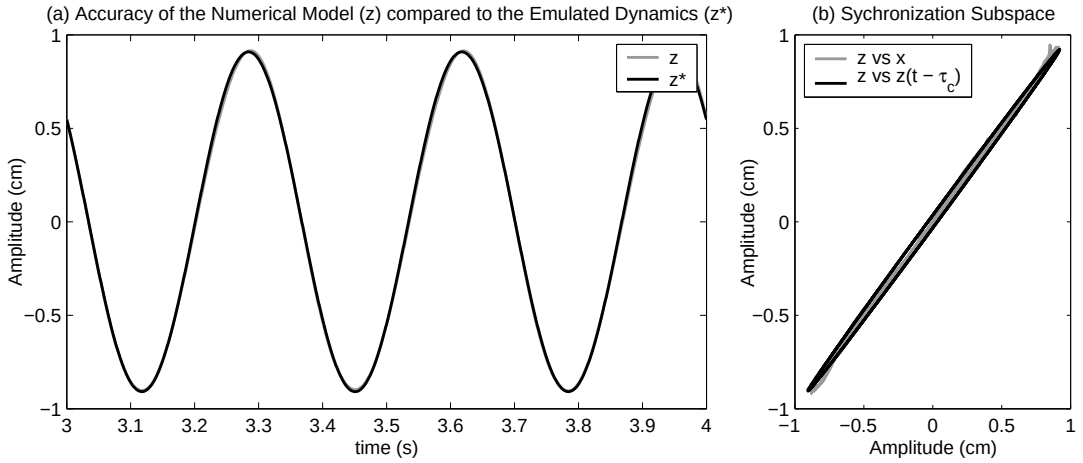

Figure 6. Experimental real-time dynamic substructure test with wall excitation of 3Hz and delay compensation of 9.4ms. Transfer system synchronisation is shown in (b) with limit of stability represented by the z vs $z(t-\tau_c)$ loop.

4.1. An over-compensation method

A fundamental difficulty for substructuring is that it is only safe to start an experimental test from a region of stability, otherwise the unstable growth may make the test impossible or damage the substructure. Hence, it is a major concern for the performance of any delay compensation algorithm to find the interval of permissible magnitudes of compensation where the substructured system is stable. Pragmatically, when starting a substructuring test for the case $\tau > \tau_c$ we can initiate the test using a numerical estimation of the force (i.e. zero time delay) and switch over to the measured force when the control algorithm has achieved a high level of synchronisation. However, ideally the test should be initiated using the measured force itself to retain the true structural characteristics.

Figure 7 demonstrates the stability restrictions imposed on the AFP algorithm by the DDE system for the two pairs of algorithm parameters N and n for a variable ρ magnitude. To this end, we use DDE-BIFTOOL to find the eigenvalues of the DDE model explicitly including the delay compensation scheme to find the forward prediction stability regions. Figure 7(a) represents the stability of the AFP algorithm for a fitting polynomial $P_{N,n,\Delta}$ of order $N = 2$ for $n = 10$ previous values of z, while Figure 7(b) corresponds to a polynomial of order $N = 4$ fitted to $n = 16$ previous values ($\Delta = 1$ms). Both prediction schemes are compared to the exact prediction (grey line) of $F = -k_s z(t + \rho - \tau)$ within the interval from -20 ms to 45 ms. If the real part of the eigenvalue is positive then the system is unstable. The dashed lines highlight the parameter value where the forward prediction equals the actual delay in the system, $\rho = \tau = 9.4$ms. The polynomial forward prediction gives, in general, only a finite interval of stability for ρ. For low order schemes the interval of permissible ρ is large. Stability ranges from $\rho \approx \tau - \tau_c = 8.065$ms to $\rho_{max} \approx 41$ ms for $N = 2$, $n = 10$ (as in Figure 7(a1)). Thus, for low N the AFP algorithm can start with an initial guess for ρ that is substantially larger than the delay τ. Increasing the order N of the fitting polynomial improves the accuracy

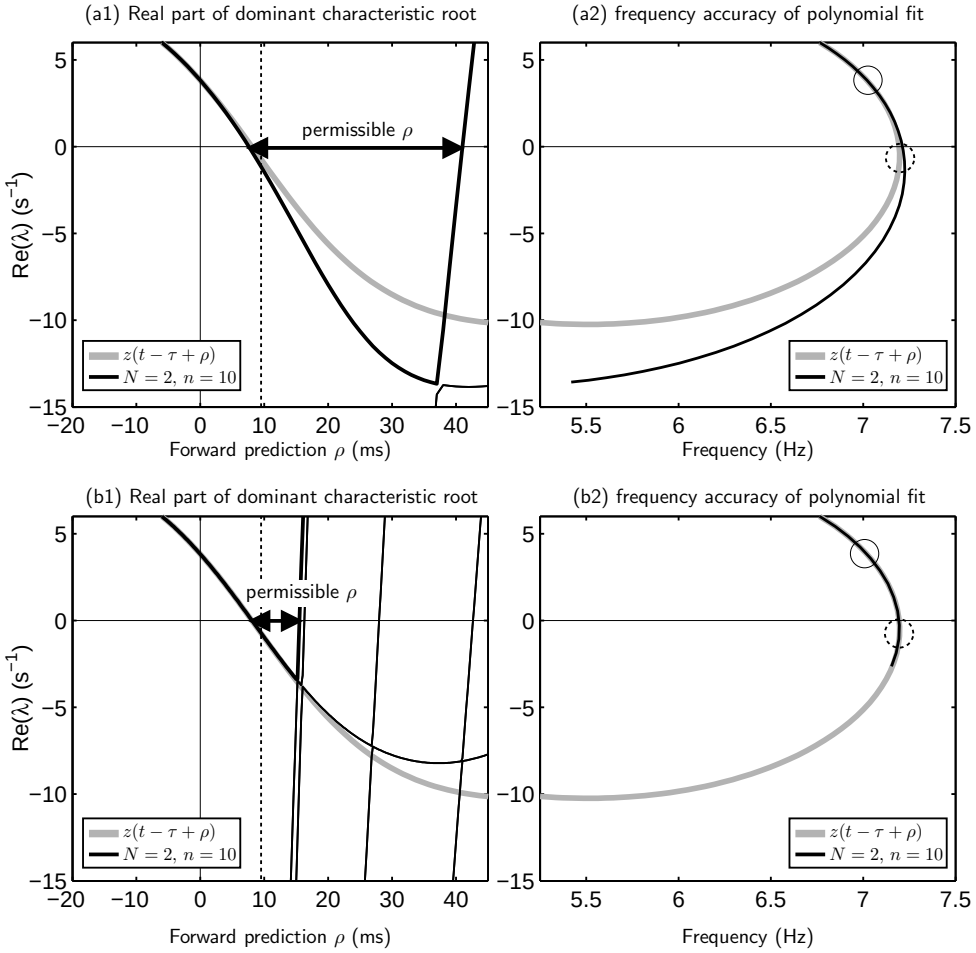

Figure 7. Eigenvalues for two delay compensation schemes compared to the exact value $z(t-\tau+\rho)$ (grey line); dominant eigenvalue is highlighted in bold. The dashed lines (circles on frequency plots) highlight where the forward prediction equals the actual delay of the transfer system, $\rho = \tau = 9.4$ms.

of the prediction as can be seen from the improved frequency accuracy of the polynomial fit shown in Figure 7(b2) compared to Figure 7(a2). However, in general, this shrinks the range of forward prediction ρ that is permissible for stability. Figure 7(b1) shows that the maximal permissible ρ is at $\rho_{\max} \approx 15\,\text{ms}$ for $N = 4$, $n = 16$. Near $\rho_{\max}$ another eigenvalue of the system becomes dominant and unstable.

Obviously, it is preferable to start the test with the optimum level of compensation, but when we do not have a good understanding of the substructure characteristics, or of the transfer system(s) we are using, it could be very difficult to estimate this value. Therefore, if the delay τ is not known and expected to be larger than the critical delay of the substructured system, the AFP algorithm should start with a low order N to give a large range of stable forward

prediction ρ and to over-compensate the initial guess, as this will give the largest stable region as shown by Figure 7. Once the adaption algorithm is close to convergence, we then increase the prediction order N to improve the accuracy of the substructuring experiment. We note that the permissible order of N is also limited by the noise fed back from the load transducer as well as $\rho_{max} > \tau - \tau_c$. Additionally, if delay is equivalent to adding negative damping in our system, then over-compensating (predicting too far forward in time) will have the opposite effect by increasing the damping. If we control to a *shifted* synchronisation origin, such that we now take $\tau = -0.5$ms as having zero synchronisation error, for example, this will have the effect of over-damping the dynamic response of the numerical model. Firstly, this makes the

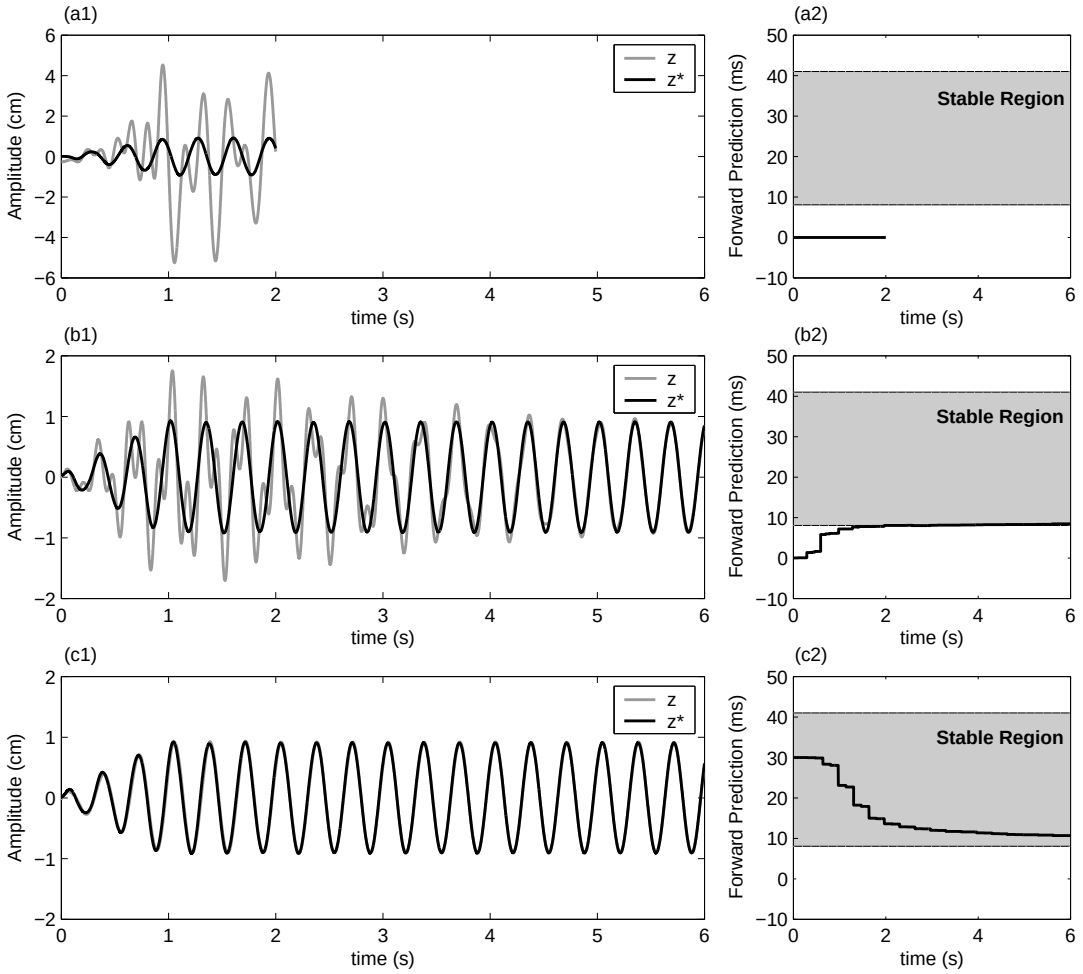

Figure 8. Experimental numerical model accuracy for differing control methodologies: (a) no delay compensation, (b) under-compensated (zero initial compensation), (c) over-compensation method (shifted synchronisation origin of $\tau = -1$ms). Controller parameters are $N = 2$, $n = 10$.

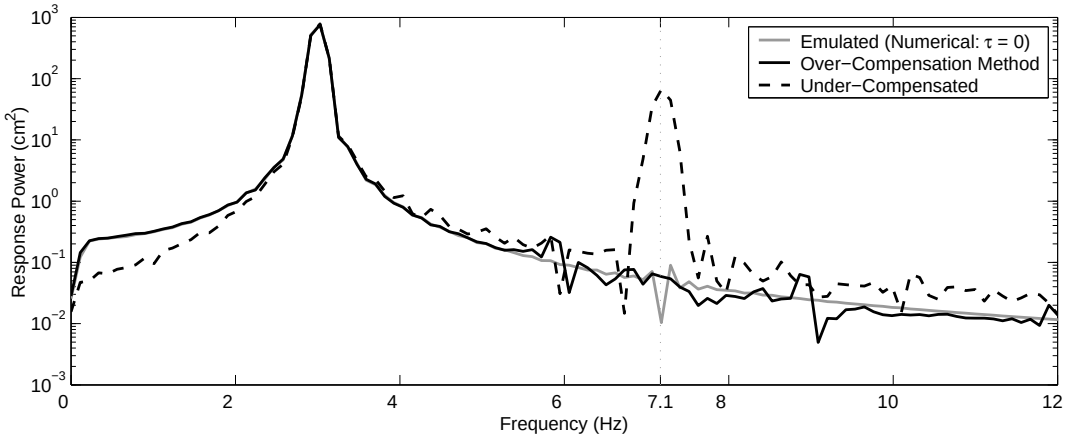

Figure 9. Comparison of the frequency spectrum for the experimental substructured responses (6s test data, see panels (b) and (c) of Figure 8) to the Emulated system.

numerical model slower to react to sudden state changes, i.e., high frequency noise fed back from the substructure, and, secondly, will mean that there is greater margin before the critical delay limit is reached. This can be seen in Figure 8, where panels (a) shows the case of no delay compensation, (b) the case for under-compensated (zero initial compensation) and (c) the over-compensation method with shifted synchronisation origin of $\tau = -1$ms.

It is noteworthy that although under-compensated, the substructured system regained stability after approximately 2s in Figure 8(b). However, once stable the unwanted oscillations take a further 3s to die out. It is not always possible for stability to be regained, in this case the controller adapts faster than the unstable growth. The consequences of such unknown dynamics could significantly affect the structural properties of the substructure and possibly lead to failure. The over-compensation method is advantageous as the substructuring algorithm is always stable (under the maximum limit) as shown in Figure 8(c2), and therefore, has a correspondingly high numerical model accuracy throughout, Figure 8(c1). The frequency at which instability is observed is shown in Figure 9. There is little difference in the spectral frequency response between the emulated dynamics (calculated numerically) and the over-compensation method (measured experimentally) whereas there is an increase of approximately three orders of magnitude at a frequency of 7.1Hz when the substructured system is under-compensated ($\omega_I = 7.1$Hz from Equation (13)). This is in contrast to the case of no delay compensation for which we see the expected exponential growth and necessity to terminate the test after 2s to prevent substructure damage in Figure 8(a1).

5. CONCLUSION

In this paper we have discussed the hybrid numerical-experimental technique of real-time dynamic substructuring. We proposed the new approach of representing the substructured system as a delay differential equation (DDE) model. This allowed us to use well established

techniques to determine the critical delay beyond which the substructured system is unstable. We used a well-known simple, linear example of a single mass-spring oscillator system to highlight the complex nature that delays play in the dynamical accuracy and stability of the substructuring algorithm. Specifically, we have demonstrated both an analytical and numerical solution for calculating the limit of stability for such a system.

In order to validate this approach experimentally, a delay compensation scheme was then used to compensate for the delay that arises through the control of the transfer system. With further numerical analysis using DDE-BIFTOOL we proposed an over-compensation method for substructuring that has a number of distinct benefits. The margin to the critical limit of stability is extend and the effects of high frequency noise are reduced. However, the primary reason for adopting such a methodology is that the test can be initiated from and entirely operated within a stable region of the substructuring algorithm. These factors become increasingly important as the damping of the structure is reduced or the stiffness is increased.

The theoretical and experimental case study presented in this paper demonstrates the overall effectiveness of the DDE modelling approach. In future work this approach will be used in more complex substructuring scenarios. The overall goal is to realize real-time dynamic substructuring of realistic engineering components, such as cables of suspension bridges and sloshing tanks for high-rise buildings, as well as for individual components such as damper units.

ACKNOWLEDGEMENTS

The research of M.I.W. is supported by an EPSRC DTA and that of J.S. by EPSRC grant GR/R72020/01. D.J.W. and B.K. are EPSRC Advanced Research Fellows.

REFERENCES

1. F.J. Molina, S. Sorace, G. Terenzi, G. Magonette, and B. Viaccoz. Seismic tests on reinforced concrete and steel frames retrofitted with dissipative braces. *Earthquake Engineering and Structural Dynamics*, 33:1373–1394, 2004.
2. M.S. Williams and A. Blakeborough. Laboratory testing of structures under dynamic loads: an introductory review. *Philosophical Transactions of the Royal Society A*, 359:1651 – 1669, 2001.
3. P.B. Shing and S.A. Mahin. Cumulative experimental errors in pseudodynamic tests. *Earthquake Engineering and Structural Dynamics*, 15:409–424, 1987.
4. M. Nakashima, H. Kato, and E. Takaoka. Development of real-time pseudo dynamic testing. *Earthquake Engineering and Structural Dynamics*, 21:779–92, 1992.
5. J. Donea, P. Magonette, P. Negro, P. Pegon, A. Pinto, and G. Verzeletti. Pseudodynamic capabilities of the ELSA laboratory for earthquake testing of large structures. *Earthquake Spectra*, 12(1):163–180, 1996.
6. O.S. Bursi and P.B. Shing. Evaluation of some implicit time-stepping algorithms for pseudodynamic tests. *Earthquake Engineering and Structural Dynamics*, 25(4):333–355, 1996.
7. M. Nakashima. Development, potential, and limitations of real-time online (pseudo dynamic) testing. *Philosophical Transactions of the Royal Society A*, 359(1786):1851–1867, 2001.
8. A. Bonelli and O.S. Bursi. Generalized-α methods for seismic structural testing. *Earthquake Engineering and Structural Dynamics*, 33(10):1067–1102, 2004.
9. A.V. Pinto, P. Pegon, G. Magonette, and G. Tsionis. Pseudo-dynamic testing of bridges using non-linear substructuring. *Earthquake Engineering and Structural Dynamics*, 33:1125–1146, 2004.
10. T. Horiuchi, M. Inoue, T. Konno, and Y. Namita. Real-time hybrid experimental system with actuator delay compensation and its application to a piping system with energy absorber. *Earthquake Engineering and Structural Dynamics*, 28:1121–1141, 1999.

11. M. Nakashima and N. Masaoka. Real-time on-line test for MDOF systems. *Earthquake Engineering and Structural Dynamics*, 28:393–420, 1999.
12. A. Blakeborough, M.S. Williams, A.P. Darby, and D.M. Williams. The development of real-time substructure testing. *Philosophical Transactions of the Royal Society of London A*, 359:1869–1891, 2001.
13. A.P. Darby, A. Blakeborough, and M.S. Williams. Real-time substructure tests using hydraulic actuator. *Journal of Engineering Mechanics*, 125(10):1133–1139, 2001.
14. P.J. Gawthrop, M.I. Wallace, and D.J. Wagg. Bond-graph based substructuring of dynamical systems. *Earthquake Engineering and Structrural Dynamics*, In press, 2004.
15. M.V. Sivaselvan, A. Reinhorn, Z. Liang, and X. Shao. Real-time dynamic hybrid testing of structural systems. *Proc. of the 13th World Conf. Earthquake Engineering*, 2004.
16. A.P. Darby, A. Blakeborough, and M.S. Williams. Improved control algorithm for real-time substructure testing. *Earthquake Engineering and Structural Dynamics*, 30:431–448, 2001.
17. D.J. Wagg and D.P. Stoten. Substructuring of dynamical systems via the adaptive minimal control synthesis algorithm. *Earthquake Engineering and Structural Dynamics*, 30:865–877, 2001.
18. C.N. Lim, S.A. Neild, D.P. Stoten, C.A. Taylor, and D. Drury. Using adaptive control for dynamic substructuring tests. *Proc. of the 3rd European Conf. on Structural Control*, 2004.
19. M.I. Wallace, D.J. Wagg, and S.A. Neild. An adaptive polynomial based forward prediction algorithm for multi-actuator real-time dynamic substructuring. *Submitted to Proceedings of the Royal Society A*, 2004.
20. O. Diekmann, S. van Gils, S.M. Verduyn Lunel, and H.O. Walther. *Delay Equations*, volume 110. 1995.
21. G. Stépan. *Retarded Dynamical Systems: Stability and Characteristic Functions*. 1989.
22. K. Engelborghs, T. Luzyanina, and D. Roose. Numerical bifurication analysis of delay differential equations using DDE-BIFTOOL. *ACM Transactions on Mathematical Software*, 28(1):1–21, 2002.
23. T. Horiuchi and T. Konno. A new method for compensating actuator delay in real-time hybrid experiments. *Philosophical Transactions of the Royal Society A*, 359:1893 – 1909, 2001.
24. T. Kalmar-Nagy, G. Stepan, and F.C. Moon. Subcritical Hopf bifurcation in the time delay equation model for machine tool vibration. *Nonlinear Dynamics*, 26:121–142, 2001.
25. D.E. Gilsinn. Estimating critical Hopf bifurcation parameters for a second order delay differential equation with application to machine tool chatter. *Nonlinear Dynamics*, 30:103–154, 2002.
26. L. Larger and J. Goedgebuer. Subcritical Hopf bifurcation in dynamical systems described by a scalar nonlinear delay differential equation. *Physical Review E*, 69(036210):1–5, 2004.
27. P. Ashwin. Non-linear dynamics, loss of synchronization and symmetry breaking. *Proceedings of the Institution of Mechanical Engineers, Part G: Journal of Aerospace Engineering*, 212(3):183–187, 1998.